

THE OFFICIAL MAGAZINE OF THE OCEANOGRAPHY SOCIETY

Oceanography

CITATION

Nguyen, A.T., V. Ocaña, V. Garg, P. Heimbach, J.M. Toole, R.A. Krishfield, C.M. Lee, and L. Rainville. 2017. On the benefit of current and future ALPS data for improving Arctic coupled ocean-sea ice state estimation. *Oceanography* 30(2):69–73, <https://doi.org/10.5670/oceanog.2017.223>.

DOI

<https://doi.org/10.5670/oceanog.2017.223>

COPYRIGHT

This article has been published in *Oceanography*, Volume 30, Number 2, a quarterly journal of The Oceanography Society. Copyright 2017 by The Oceanography Society. All rights reserved.

USAGE

Permission is granted to copy this article for use in teaching and research. Reproduction, systematic reproduction, or collective redistribution of any portion of this article by photocopy machine, reposting, or other means is permitted only with the approval of The Oceanography Society. Send all correspondence to: info@tos.org or The Oceanography Society, PO Box 1931, Rockville, MD 20849-1931, USA.

On the Benefit of Current and Future ALPS Data for Improving Arctic Coupled Ocean-Sea Ice State Estimation

By An T. Nguyen, Victor Ocaña, Vikram Garg, Patrick Heimbach, John M. Toole, Richard A. Krishfield, Craig M. Lee, and Luc Rainville

ABSTRACT. Autonomous and Lagrangian platforms and sensors (ALPS) have revolutionized the way the subsurface ocean is observed. The synergy between ALPS-based observations and coupled ocean-sea ice state and parameter estimation as practiced in the Arctic Subpolar gyre State Estimate (ASTE) project is illustrated through several examples. In the western Arctic, Ice-Tethered Profilers have been providing important hydrographic constraints of the water column down to 800 m depth since 2004. ASTE takes advantage of these detailed constraints to infer vertical profiles of diapycnal mixing rates in the central Canada Basin. The state estimation framework is also used to explore the potential utility of Argo-type floats in regions with sparse data coverage, such as the eastern Arctic and the seasonal ice zones. Finally, the framework is applied to identify potential deployment sites that optimize the impact of float measurements on bulk oceanographic quantities of interest.

INTRODUCTION

The ability to sample the interior ocean at dense spatial coverage and continuously on seasonal to multidecadal time scales is a prerequisite for improved understanding of the ocean's mean state, variability, and long-term change. Since the early 2000s, autonomous and Lagrangian platforms and sensors (ALPS) have contributed significantly to the way the ocean is observed in the lower latitudes and coastal regions (Riser et al., 2016; Rudnick, 2016). At high latitudes, the Arctic Ocean has become increasingly more observable, with new data sets from satellite altimetry (e.g., Laxon et al., 2013), gravimetry (Watkins et al., 2015), in situ Ice-Tethered Profilers (ITP, measuring subsurface hydrography; Krishfield et al., 2008; Timmermans et al., 2008; Toole et al., 2011), and a variety of sensors on autonomous platforms (Lee et al., 2010, and Lee and Thomson, 2017, in this issue). One powerful way to integrate these vastly heterogeneous (in space and time) streams of in situ and remote-sensing observations is to produce an Arctic ocean-sea ice synthesis using existing ocean-ice data assimilation or state estimation frameworks (Wunsch and Heimbach, 2007). Edwards et al. (2015) and Stammer et al. (2016) provide lists of regional and global examples of ocean data assimilation, and discuss the advantages and disadvantages of filter- versus smoother-based assimilation frameworks, with a key difference being that in the smoother framework, the equations of motion, for example, conservation laws, are strictly obeyed (i.e., no mass, momentum, or heat can be artificially created or destroyed). Data assimilation focusing on sea ice in polar regions is covered at length in Carrieres et al. (in press).

One such smoother-based framework is that developed within the Estimation of the Circulation and Climate of the Ocean (ECCO) consortium (Stammer et al., 2002; Wunsch and Heimbach, 2007, 2013; Forget et al., 2015a). In this paper, we briefly introduce the ECCO framework as a computational tool for constructing a dynamically evolving Arctic ocean-sea ice state estimate through data-model synthesis. We present a specific example focusing on how existing ITP data can be used to adjust the model internal mixing parameters to bring the synthesis into consistency with observations. Where there is currently a shortage of data coverage to

constrain the state estimate, such as in the eastern Arctic, we show how ECCO inversion-based sensitivity tools can be applied to aid the identification of “optimal” sites where new ALPS-type instruments can potentially be deployed.

THE ARCTIC SUBPOLAR GYRE STATE ESTIMATE (ASTE)

The ECCO state estimation framework combines all available observations with a general circulation model in a way that maximizes the data contribution as model constraints while preserving the underlying model physics. As an extension of the global ECCO state estimate, a regional medium-resolution Arctic Subpolar gyre State Estimate (ASTE) has been developed to emphasize the northern high-latitude regions. ASTE uses the Massachusetts Institute of Technology general circulation model (MITgcm) and its adjoint (Marshall et al., 1997; Adcroft et al., 2004). The state estimate is obtained through weighted least-squares minimization of the observation-model misfits while strictly adhering to the underlying model equations of motion, which permit accurate circulation and budget analyses (Wunsch and Heimbach, 2007; Stammer et al., 2016). Adjustable parameters in ASTE include initial hydrography, three-dimensional mixing parameters, and atmospheric forcing. ASTE's primary goal is to reconstruct the ocean and sea ice time-mean and evolving state in the early twenty-first century for use in high-latitude climate research (see next section). In addition, ASTE can be used to aid observing network design (see section on The Need for Additional ALPS Data).

ITP DATA AS CONSTRAINTS FOR ESTIMATING OCEAN MODEL PARAMETERS

Molecular and turbulent diffusion dominate in the ocean's interior, away from the surface, boundary currents, and regions with significant seafloor topography. In addition to turbulent diffusion, eddy stirring mixes temperature and salinity (T, S) along constant density layers (e.g., Ledwell et al., 1993; Watson et al., 2013). Together with advection, these mixing processes redistribute heat and salt, help to maintain ocean stratification, and contribute to the global overturning circulation (Munk, 1966; Munk and Wunsch, 1998; Killworth, 1998; Kunze et al., 2006). Despite their importance, knowledge of the three-dimensional distribution (and time-dependence) of these mixing fields is severely limited due to lack (until recently) of direct observations. For vertical turbulent and molecular mixing, measurements of T, S, and velocities at vertical spatial scales of centimeters are required throughout the entire water column and at horizontal spacing spanning the entire ocean, a suite of measurements not easy to collect (Killworth, 1998). In the absence of direct observations, mixing fields are often inferred from indirect observations and theories (e.g., Kunze et al., 2006; Whalen et al., 2012; Cole et al., 2015). At high latitudes, lack of knowledge in the three-dimensional distribution of these mixing fields is one of the primary reasons the Arctic Ocean's mean horizontal and vertical hydrographic structure is not well reproduced in numerical models (Holloway et al., 2007; Nguyen et al., 2011; Illicak et al., 2016).

One of ASTE's goals is to take advantage of existing subsurface ALPS observations to improve estimates of pan-Arctic

three-dimensional mixing parameters, following the methodology of Stammer (2005), Liu et al. (2012), and Forget et al. (2015b). It is possible to invert for model internal parameters, in particular those related to active tracer mixing, if there are data with good temporal and spatial coverage, and if the parameters are smooth functions of ocean hydrographic properties. When these conditions are not met (e.g., sparse data coverage in the eastern Arctic and the marginal ice zones), the inversion for a full three-dimensional field is highly under-determined (i.e., there is no unique solution for mixing value at each model grid point). Given the limited spatial and temporal sampling, our first approach is to reduce the number of dimensions and

investigate basin-scale mean vertical mixing rates. That is, we seek to address the first-order question of what the required distribution of vertical diffusivity should be to maintain the observed vertical density (salinity) structure.

The observational data used to invert for vertical mixing rates come from ITPs, which at present offer the best available temporal and regional coverage of the upper 800 m of the water column below sea ice in the western Arctic (Figure 1). More than one-third of available ITP temperature and salinity profiles are concentrated in the Canada Basin (Figure 1a). This spatial distribution offers an ideal place to invert for the mean vertical mixing κ_z in a one-dimensional

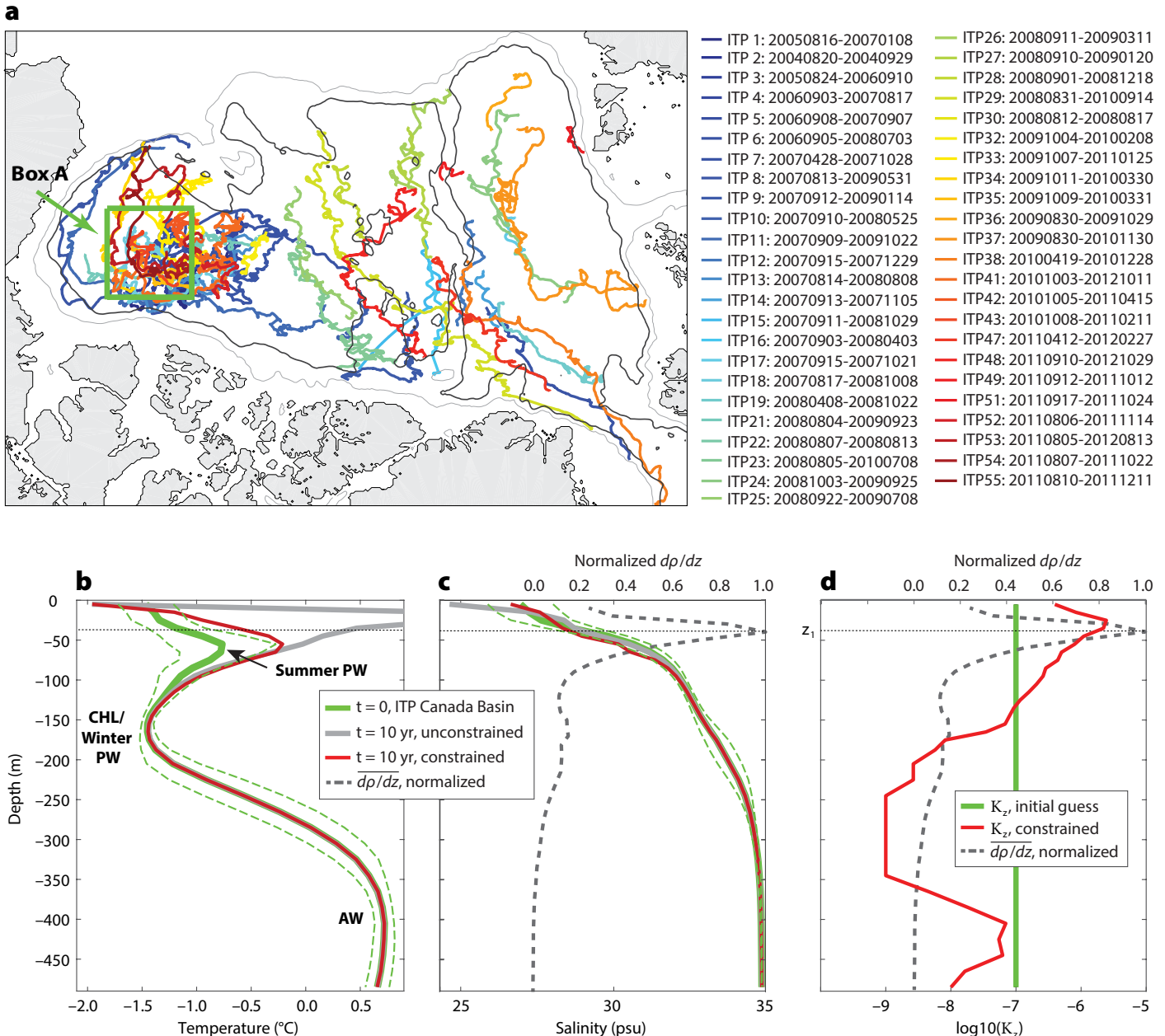


FIGURE 1. (a) Ice-Tethered Profiler (ITP) data available for the period 2004–2012 used to constrain the Arctic Subpolar gyre sTate Estimate (ASTE). Data in Box A are used to infer the box-mean ocean vertical mixing rate in the upper 800 m of the water column. Lower panels display vertical profiles of (b) temperature, (c) salinity, and (d) vertical diffusivity κ_z at model time $t = 0$ (green) and $t = 10$ years (gray, red) in a one-dimensional column setup. Initial temperature and salinity (T, S) conditions are set to the mean of Box A shown in (a). Atmospheric forcing is from the Japanese 55-year Reanalysis (JRA-55, Kobayashi et al., 2015) 2002–2015 monthly mean climatology. Data and representation errors in T and S are obtained from Box A's standard deviations (STD, dashed green). In the unconstrained run, with an initial guess $\kappa_z = 10^{-7} \text{ m}^2 \text{ s}^{-1}$ at all depths, the upper ocean (above z_1) is too stratified with not enough vertical diffusion to redistribute the extra heat absorbed from the atmosphere during each summer (gray lines). With Box A's T, S constraints, a new inverted vertical profile of κ_z obtained from the inversion procedure (red curve in panel d) brings the model temperature and salinity into agreement with Box A's observations, within the error bars (red curves in b–c). After 18 iterations, the model–ITP misfits are reduced by roughly 77%.

column configuration (Figure 1b,c). Horizontal advection and diffusion were ignored in this initial estimation step. The mean of all ITP profiles covering the period 2004–2012 within Box A (Figure 1a) was used to establish initial temperature and salinity. Box A's temperature and salinity mean and standard deviations were also used as daily observational constraints and uncertainties, respectively.

Based on previous numerical studies (Zhang and Steele, 2007; Nguyen et al., 2011), a first-guess value for κ_z was set at $10^{-7} \text{ m}^2 \text{ s}^{-1}$, with an uncertainty of $10^{-5} \text{ m}^2 \text{ s}^{-1}$ to allow for adjustments to either enhance or decrease mixing as required to maintain the vertical water column structure. The one-dimensional column model was first integrated for 10 years without applying data constraints. Then, κ_z was iteratively improved from its initial guess using temperature and salinity as constraints. After 18 iterations, the model-data misfits were reduced by 77%. A closer inspection shows that the constant value of κ_z used as a first guess limited mixing in the upper 50 m of the ocean and resulted in the summer heat absorbed from the atmosphere being trapped just below the surface. In contrast, the new depth-dependent estimate of κ_z (Figure 1d), with higher values above 100 m and lower values at the interfaces between the Atlantic Water and the cold halocline, allows for the modeled temperature and salinity to be in agreement with the observations to within the data uncertainty (red curves in Figure 1b,c). Note that deviations between the modeled and observed temperature and salinity can still remain, but because the normalized misfits, defined as the absolute values of $([T,S]_{\text{model}} - [T,S]_{\text{observed}})/\text{error}_{[T,S]}$, are now at or below one, the inversion has converged with an optimized κ_z . Also note that the model's temperature and salinity evolve consistently with the model physics subject to external forcing at the surface, and only the time-mean input vertical mixing parameter is updated based on the information provided by temperature and salinity data.

In the Arctic Ocean's interior, the prevalence of horizontal staircase structures associated with double diffusion in the observed basin-scale T, S vertical profiles suggests that horizontal advection and eddy stirring are not strong enough to destroy these staircases (Padman and Dillon, 1987; Timmermans et al., 2008; Fer, 2009; Polyakov et al., 2011; Bebieva and Timmermans, 2016). This lends support to the omission of these horizontal processes in our one-dimensional approximation. Near regions with significant seafloor topography and along boundary currents, advection and horizontal diffusion can enhance vertical mixing and need to be taken into account when estimating κ_z (Padman and Dillon, 1987; Timmermans et al., 2008). Lastly, near the surface, the time-mean inverted κ_z estimated here is not applicable, and the model uses a separate boundary layer parameterization.

THE NEED FOR ADDITIONAL ALPS DATA FOR OBSERVING-NETWORK DESIGN

The ITP data set has significantly improved our knowledge of subsurface processes in the central Arctic and permits inversion of vertical mixing rates in the Canada Basin; however, a major limiting factor is that its sampling is confined to ice-covered regions. The reduced data coverage in the eastern Arctic and along Atlantic Waters (AW) boundary current pathways leaves the hydrography upstream of the Canada Basin essentially unconstrained. Using ASTE, we explore the potential utility of Arctic "Argo-type" floats (Riser et al., 2016) to improve estimates of the Arctic mean hydrography and model internal parameters through observing system simulation experiments (OSSEs). In doing so, we account for the possibility that such floats are not able to resurface for extended time periods while profiling under sea ice, as well as for lack of knowledge of the mean Arctic circulation. Implied position uncertainties of profiles so obtained and stored until the next resurfacing are translated into hydrographic uncertainties. Our primary goals are to quantify this hydrographic uncertainty

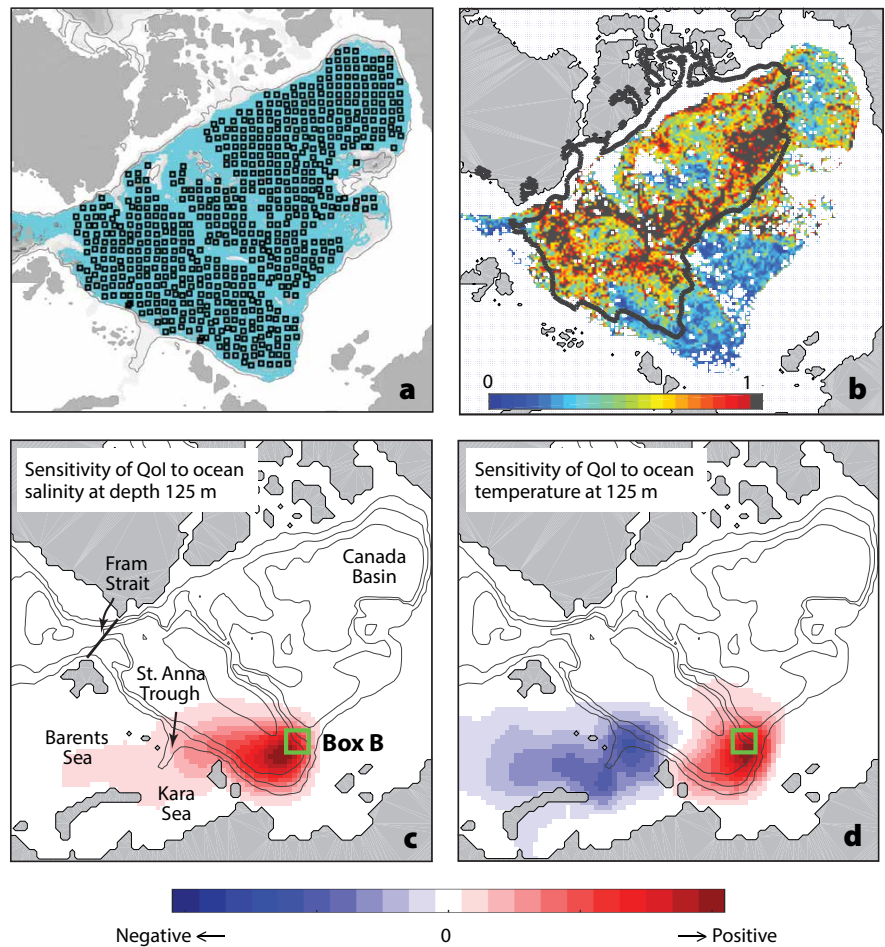
and to assess whether circulation estimates obtained through assimilating these data in ASTE can improve our knowledge of uncertain positions during times when the floats have not surfaced.

An OSSE was configured with 681 synthetic Argo floats distributed throughout the deep Arctic (Figure 2a) to collect "true" temperature and salinity. An additional 200 experiments, each with 681 floats with noise added to the mean flow field, were simulated for a five-year period to build the position and T, S misfit database. The spatial distribution of these 681 floats is such that they cover the entire Arctic deep basin at a nominal separation distance of 70 km (every fourth grid point in ASTE). T, S misfits are then calculated between the "true" and simulated fields, normalized by the combined observation uncertainty and model representation errors (Forget and Wunsch, 2007; Fenty and Heimbach, 2013). The pattern of T, S errors follows the summer minimum sea ice distribution, an expected result given that the presence of sea ice is the limiting factor in a float being able to surface (Figure 2b). When nearby underwater acoustic sources exist, such as those currently being implemented by the US Office of Naval Research (ONR) in the western Arctic or international efforts in the Fram Strait region (Mikhalevsky et al., 2015), they will be used for acoustic navigation (Jones et al., 2013; Schmidt and Schneider, 2016) to further reduce errors in float positions and hydrographic measurements.

A deployment of a uniform and dense array of Argo-type floats in the Arctic is currently unrealistic. Given limited resources, the ASTE adjoint sensitivity tool (e.g., Heimbach et al., 2011; Pillar et al., 2016) can be used to identify optimal sites for float deployments in data-deficient regions such as the eastern Arctic as follows. First, a target quantity of interest (QoI), such as the mean salinity of Box B within a depth range covering the AW layer (145–250 m, green box in Figure 2c), is defined. We seek to determine where instruments should be deployed to improve knowledge of this QoI. The ASTE adjoint model is used to calculate the spatial distribution of sensitivity of the QoI to ocean three-dimensional T, S back in time (Figure 2c,d). These sensitivity maps provide temporal and spatial information useful for guiding float deployment upstream of the target Box B (Figure 2c,d). For this example QoI, any region of non-zero sensitivity is identified as a region of influence, such that a float deployed there has the potential to transit Box B approximately 36 months later. In addition, the sign of the sensitivity provides information on Box B's variability, such that a positive (negative) sensitivity implies Box B's mean salinity will likely be higher (lower) than its mean value. In addition, any acoustic source/receiver within the non-zero sensitivity region can potentially be used by the float for acoustic positioning as it travels along its path. The 36-month period shown in Figure 2c,d is only chosen to illustrate the pattern of sensitivity for this time lag. Depending on logistics, floats can potentially be deployed further upstream or downstream along the expected mean AW flow path. The expected time of arrival in the vicinity of Box B will be longer or shorter than 36 months, respectively.

Here, we have discussed potential new deployment of Argo-type floats in the deep Arctic basin at depths >1,000 m. Recent deployments in the Baltic Sea demonstrate that Argo-type floats can operate well and yield high-quality data in water as shallow as 50 m (Purokoski et al., 2013; Westerlund and Tuomi, 2016). Thus, the adjoint sensitivity methodology discussed here can also be applied to seasonally ice-covered marginal seas in the Arctic. Depending on the circulation and time scale of residence in the sea, a float can potentially either survive a full ice-covered season and surface to relay data during the ice-free period, or be advected into the deep ocean (e.g., Figure 2 with a deployment in the Kara Sea, drifting through the Santa Anna Trough into the eastern Arctic).

FIGURE 2. (a) Initial distribution of synthetic floats (black squares) and all their trajectories (cyan) after a five-year model simulation. (b) Mean normalized error in salinity within depth range 100–300 m. Error accumulates when a float operates under sea ice and cannot determine its position by satellite. Where error is <1, the float measurements are considered “useful” in improving the mean salinity estimate, reducing its uncertainty. The black contour shows the model simulated 1992–2010 mean sea ice minimum. (c–d) Adjoint sensitivity of a quantity of interest (QoI), here defined as Box B monthly mean salinity in the depth range 140–250 m of the water column, to (c) ocean salinity and (d) temperature changes at a depth 125 m at 36 months prior. If the objective of a float deployment is to improve knowledge of the salinity in Box B, any region upstream of Box B with non-zero sensitivity is a potential deployment site. In addition, the sign of the sensitivity (positive or negative) also provides information about the potential variability measured at Box B. For example (panel d), if a float is deployed in the Kara Sea and measures a negative anomaly in temperature relative to a local time-mean value, we anticipate that approximately 36 months later the float will likely transit to nearby or through Box B and that the measured salinity at Box B will likely be above its time-mean background value. Now looking at (c), if a measurement of salinity from a float deployed near the St. Anna Trough is above its time-mean local values, we also anticipate that 36 months later that float will transit near Box B or through it, and the measurement taken at that time would yield a positive salinity anomaly at Box B relative to its time-mean background value.



OUTLOOK

The ability to sample the ocean’s interior globally and continuously on seasonal to multidecadal time scales is a prerequisite for improved understanding of the ocean’s mean state, its variability, and its secular changes. A state estimation framework that combines observations with a state-of-the-art numerical model, while strictly adhering to the underlying conservation equations, can help infer the mechanisms responsible for changing heat, salt, and freshwater budgets. Currently available ALPS data have been heavily utilized within the ECCO framework to improve estimates of the time-evolving global ocean-sea ice state on decadal time scales (Wunsch and Heimbach, 2013; Forget et al., 2015a).

The presence of sea ice in the Arctic has limited the deployment of ALPS-type sensors and the interpretation of subsurface measurements that would help improve high-latitude ocean-sea ice state estimation. Nevertheless, with recent technological advances in float design, Argo-type instruments can now be deployed under seasonally ice-covered regions (Wong and Riser, 2011; Riser et al., 2016). In addition, underwater acoustic network developments by ONR (Lee et al., 2012; Freitag et al., 2015) and other international efforts (Mikhalevsky et al., 2015) offer excellent opportunities for testing float acoustic navigation (Jones et al., 2013; Schmidt and Schneider, 2016) toward potentially alleviating the sea ice challenge. With these new developments, a strong synergy between observations and ASTE can be established: new subsurface observations can be used to improve ASTE, and in turn, ASTE with its adjoint sensitivity tools can help inform float-deployment design in order to minimize observational errors and maximize the impact of data collected in improvement of Arctic ocean-sea ice state estimates. ☑

REFERENCES

- Adcroft, A., C. Hill, J.-M. Campin, J. Marshall, and P. Heimbach. 2004. Overview of the formulation and numerics of the MIT GCM. Pp. 139–150 in *Seminar on Recent Developments in Numerical Methods for Atmospheric and Ocean Modelling*. September 6–10, 2004, ECMWF, Shinfield Park, Reading.
- Bebieva, Y., and M.-L. Timmermans. 2016. An examination of double-diffusive processes in a mesoscale eddy in the Arctic Ocean. *Journal of Geophysical Research* 121:457–475, <https://doi.org/10.1002/2015JC011105>.
- Carrieres, T., M. Buehner, J.-F. Lemieux, and L.T. Pedersen. In press. *Sea Ice Analysis and Forecasting*. Cambridge University Press, Cambridge, UK.
- Cole, S., C. Wortham, E. Kunze, and W. Owens. 2015. Eddy stirring and horizontal diffusivity from Argo float observations: Geographic and depth variability. *Geophysical Research Letters* 42:3,989–3,997, <https://doi.org/10.1002/2015GL063827>.
- Edwards, C.A., A.M. Moore, I. Hoteit, and B.D. Cornuelle. 2015. Regional ocean data assimilation. *Annual Review of Marine Science* 7(1):21–42, <https://doi.org/10.1146/annurev-marine-010814-015821>.
- Fenty, I., and P. Heimbach. 2013. Coupled sea ice–ocean-state estimation in the Labrador Sea and Baffin Bay. *Journal of Physical Oceanography* 43:884–904, <https://doi.org/10.1175/JPO-D-12-065.1>.
- Fer, I. 2009. Weak vertical diffusion allows maintenance of cold halocline in the Central Arctic. *Atmospheric and Oceanic Science Letters* 2:148–152, <https://doi.org/10.1080/16742834.2009.11446789>.
- Forget, G., J. Campin, P. Heimbach, C. Hill, R. Ponte, and C. Wunsch. 2015a. ECCO version 4: An integrated framework for non-linear inverse modeling and global ocean state estimation. *Geoscientific Model Development* 8:3,071–3,104, <https://doi.org/10.5194/gmd-8-3071-2015>.
- Forget, G., D. Ferreira, and X. Liang. 2015b. On the observability of turbulent transport rates by Argo: Supporting evidence from an inversion experiment. *Ocean Science* 11:839–853, <https://doi.org/10.5194/os-11-839-2015>.
- Forget, G., and C. Wunsch. 2007. Estimated global hydrographic variability. *Journal of Physical Oceanography* 37(8):1,997–2,008, <https://doi.org/10.1175/JPO3072.1>.
- Freitag, L., K. Ball, J. Partan, P. Koski, and S. Singh. 2015. Long range acoustic communications and navigation in the Arctic. Pp. 1–5 in *2015 MTS/IEEE OCEANS*, Washington, DC, <https://doi.org/10.23919/OCEANS.2015.7401956>.

- Heimbach, P., C. Wunsch, R.M. Ponte, G. Forget, C. Hill, and J. Utke. 2011. Timescales and regions of the sensitivity of Atlantic meridional volume and heat transport: Toward observing system design. *Deep Sea Research Part II* 58:1,858–1,879, <https://doi.org/10.1016/j.dsr2.2010.10.065>.
- Holloway, G., F. Dupont, E. Golubeva, S. Hakkinen, E. Hunke, M. Jin, M. Karcher, F. Kauker, M. Maltrud, M.M. Maqueda, and others. 2007. Water properties and circulation in Arctic Ocean models. *Journal of Geophysical Research* 112, C04S03, <https://doi.org/10.1029/2006JC003642>.
- Ilicak, M., H. Drange, Q. Wang, R. Gerdes, Y. Aksenov, D. Bailey, M. Bentsen, A. Biastoch, A. Bozec, C. Böning, and others. 2016. An assessment of the Arctic Ocean hydrography in a suite of interannual CORE-II simulations: Part III. Hydrography and fluxes. *Ocean Modelling* 100:141–161, <https://doi.org/10.1016/j.ocemod.2016.02.004>.
- Jones, C., A. Morozov, and J.E. Manley. 2013. Under ice positioning and communications for unmanned vehicles. Pp. 1–6 in *2013 MTS/IEEE OCEANS - Bergen*, <https://doi.org/10.1109/OCEANS-Bergen.2013.6607978>.
- Killworth, P. 1998. Something stirs in the deep. *Nature* 396:720–721, <https://doi.org/10.1038/25444>.
- Kobayashi, S., Y. Ota, Y. Harada, A. Ebata, M. Moriya, H. Onoda, K. Onogi, H. Kamahori, C. Kobayashi, H. Endo, and others. 2015. The JRA-55 reanalysis: General specifications and basic characteristics. *Journal of the Meteorological Society of Japan* 93:5–48, <https://doi.org/10.2151/jmsj.2015-001>.
- Krishfield, R., J. Toole, A. Proshutinsky, and M.-L. Timmermans. 2008. Automated Ice-Tethered Profilers for seawater observations under pack ice in all seasons. *Journal of Atmospheric and Oceanic Technology* 25:2,091–2,105, <https://doi.org/10.1175/2008JTECHO5871>.
- Kunze, E., E. Firing, J. Hummon, T. Chereskin, and A. Thurnherr. 2006. Global abyssal mixing inferred from lowered ADCP shear and CTD strain profiles. *Journal of Physical Oceanography* 36:1,553–1,576, <https://doi.org/10.1175/JPO29261>.
- Laxon, S., K. Giles, A. Ridout, D. Wingham, R. Willatt, R. Cullen, R. Kwok, A. Schweiger, J. Zhang, C. Haas, and others. 2013. CryoSat-2 estimates of Arctic sea ice thickness and volume. *Geophysical Research Letters* 40:732–737, <https://doi.org/10.1002/grl.50193>.
- Ledwell, J., A. Watson, and C. Law. 1993. Evidence for slow mixing across the pycnocline from an open-ocean tracer-release experiment. *Nature* 364:701–703, <https://doi.org/10.1038/364701a0>.
- Lee, C.M., S. Cole, M. Doble, L. Freitag, P. Hwang, S. Jayne, M. Jeffries, R. Krishfield, T. Maksym, W. Maslowski, and others. 2012. *Marginal Ice Zone (MIZ) Program: Science and Experiment Plan*. Technical Report APL/UW 1201. Applied Physics Laboratory, University of Washington, Seattle, 48 pp.
- Lee, C.M., H. Melling, H. Eicken, P. Schlosser, J.-C. Gascard, A. Proshutinsky, E. Fahrbach, C. Mauritzen, J. Morison, and I. Polyakov. 2010. Autonomous platforms in the Arctic Observing Network. *Proceedings of OceanObs09: Sustained Ocean Observations and Information for Society*, vol. 2. Venice, Italy, September 21–25, 2009. J. Hall, D. Harrison, and D. Stammer, eds, ESA, <https://doi.org/10.5270/OceanObs09.cwp.54>.
- Lee, C.M., J. Thomson, and the Marginal Ice Zone and Arctic Sea State Teams. 2017. An autonomous approach to observing the seasonal ice zone in the western Arctic. *Oceanography* 30(2):56–68, <https://doi.org/10.5670/oceanog.2017.222>.
- Liu, C., A. Köhl, and D. Stammer. 2012. Adjoint-based estimation of eddy-induced tracer mixing parameters in the global ocean. *Journal of Physical Oceanography* 42:1,186–1,206, <https://doi.org/10.1175/JPO-D-11-0162.1>.
- Marshall, J., A. Adcroft, C. Hill, L. Perelman, and C. Heisey. 1997. A finite-volume, incompressible Navier Stokes model for studies of the ocean on parallel computers. *Journal of Geophysical Research* 102:5,753–5,766, <https://doi.org/10.1029/96JC02775>.
- Mikhalevsky, P., H. Sagen, P. Worcester, A. Baggeroer, J. Orcutt, S. Moore, C. Lee, K. Vigness-Raposa, L. Freitag, M. Arrott, and others. 2015. Multipurpose acoustic networks in the integrated Arctic Ocean observing system. *ARCTIC* 68:11–27, <https://doi.org/10.14430/arctic4449>.
- Munk, W.H. 1966. Abyssal recipes. *Deep Sea Research Part I* 13:707–730, [https://doi.org/10.1016/0011-7471\(66\)90602-4](https://doi.org/10.1016/0011-7471(66)90602-4).
- Munk, W., and C. Wunsch. 1998. Abyssal recipes II: Energetics of tidal and wind mixing. *Deep Sea Research Part I* 45:1,977–2,010, [https://doi.org/10.1016/S0967-0637\(98\)00070-3](https://doi.org/10.1016/S0967-0637(98)00070-3).
- Nguyen, A.T., D. Menemenlis, and R. Kwok. 2011. Arctic ice-ocean simulation with optimized model parameters: Approach and assessment. *Journal of Geophysical Research* 116, C04025, <https://doi.org/10.1029/2010JC006573>.
- Padman, L., and T.M. Dillon. 1987. Vertical heat fluxes through the Beaufort Sea thermohaline staircase. *Journal of Geophysical Research* 92:10,799–10,806, <https://doi.org/10.1029/JC092iC10p10799>.
- Pillar, H.R., P. Heimbach, H.L. Johnson, and D.P. Marshall. 2016. Dynamical attribution of recent variability in Atlantic overturning. *Journal of Climate* 29:3,339–3,352, <https://doi.org/10.1175/JCLI-D-15-0727.1>.
- Polyakov, I.V., A.V. Pnyushkov, R. Rember, V.V. Ivanov, Y.-D. Lenn, L. Padman, and E.C. Carmack. 2011. Mooring-based observations of double-diffusive staircases over the Laptev Sea slope. *Journal of Physical Oceanography* 42:95–109, <https://doi.org/10.1175/2011JPO4606.1>.
- Purokoski, T., E. Aro, and A. Nummelin. 2013. First long-term deployment of Argo float in Baltic Sea. *Sea Technology* 54:41–44.
- Riser, S.C., H.J. Freeland, D. Roemmich, S. Wijffels, A. Troisi, M. Belbeoch, D. Gilbert, J. Xu, S. Pouliquen, A. Thresher, and others. 2016. Fifteen years of ocean observations with the global Argo array. *Nature Climate Change* 6:145–153, <https://doi.org/10.1038/NCLIMATE2872>.
- Rudnick, D.L. 2016. Ocean research enabled by underwater gliders. *Annual Review of Marine Science* 8:519–541, <https://doi.org/10.1146/annurev-marine-122414-033913>.
- Schmidt, H., and T. Schneider. 2016. Acoustic communication and navigation in the new Arctic: A model case for environmental adaptation. Pp. 1–4 in *2016 IEEE Third Underwater Communications and Networking Conference (UComms)*, <https://doi.org/10.1109/UComms.2016.7583469>.
- Stammer, D. 2005. Adjusting internal model errors through ocean state estimation. *Journal of Physical Oceanography* 35:1,143–1,153, <https://doi.org/10.1175/JPO2733.1>.
- Stammer, D., M. Balmaseda, P. Heimbach, A. Köhl, and A. Weaver. 2016. Ocean data assimilation in support of climate applications: Status and perspectives. *Annual Review of Marine Science* 8:491–518, <https://doi.org/10.1146/annurev-marine-122414-034113>.
- Stammer, D., C. Wunsch, R. Giering, C. Eckert, P. Heimbach, J. Marotze, A. Adcroft, C.N. Hill, and J. Marshall. 2002. Global ocean circulation during 1992–1997, estimated from ocean observations and a general circulation model. *Journal of Geophysical Research* 107(C9), 3118, <https://doi.org/10.1029/2001JC000888>.
- Timmermans, M.-L., J. Toole, R. Krishfield, and P. Winsor. 2008. Ice-Tethered Profiler observations of the double-diffusive staircase in the Canada Basin thermocline. *Journal of Geophysical Research*, 113, C00A02, <https://doi.org/10.1029/2008JC004829>.
- Toole, J.M., R.A. Krishfield, and M.-L. Timmermans. 2011. The Ice-Tethered Profiler: Argo of the Arctic. *Oceanography* 24(3):126–135, <https://doi.org/10.5670/oceanog.2011.64>.
- Watkins, M., D. Wiese, D.-N. Yuan, C. Boening, and F. Landerer. 2015. Improved methods for observing Earth's time variable mass distribution with GRACE using spherical cap mascons. *Journal of Geophysical Research* 120:2,648–2,671, <https://doi.org/10.1002/2014JB011547>.
- Watson, A., J. Ledwell, M.-J. Messias, B. King, N. Mackay, M. Meredith, B. Mills, and A. Garabato. 2013. Rapid cross-density ocean mixing at mid-depths in the Drake Passage measured by tracer release. *Nature* 501:408–411, <https://doi.org/10.1038/nature12432>.
- Westerlund, A., and L. Tuomi. 2016. Vertical temperature dynamics in the northern Baltic Sea based on 3D modelling and data from shallow-water Argo floats. *Journal of Marine Systems* 158:34–44, <https://doi.org/10.1016/j.jmarsys.2016.01.006>.
- Whalen, C.B., L.D. Talley, and J.A. MacKinnon. 2012. Spatial and temporal variability of global ocean mixing inferred from Argo profiles. *Geophysical Research Letters* 39, L18612, <https://doi.org/10.1029/2012GL053196>.
- Wong, A.P.S., and S.C. Riser. 2011. Profiling float observations of the upper ocean under sea ice off the Wilkes Land coast of Antarctica. *Journal of Physical Oceanography* 41:1,102–1,115, <https://doi.org/10.1175/2011JPO4516.1>.
- Wunsch, C., and P. Heimbach. 2007. Practical global oceanic state estimation. *Physica D* 230:197–208, <https://doi.org/10.1016/j.physd.2006.09.040>.
- Wunsch, C., and P. Heimbach. 2013. Dynamically and kinematically consistent global ocean circulation and ice state estimates. Pp. 553–579 in *Ocean Circulation and Climate: A 21st Century Perspective*. G. Siedler, S. Griffies, J. Gould, and J. Church, eds, vol. 103 of International Geophysics, Oxford, UK, Academic Press.
- Zhang, J., and M. Steele. 2007. Effect of vertical mixing on the Atlantic Water layer circulation in the Arctic Ocean. *Journal of Geophysical Research* 112, C04S04, <https://doi.org/10.1029/2006JC003732>.

ACKNOWLEDGMENTS

This research was supported by NSF Grants PLR-1643339, PLR-1603903, and PLR-1603660. Sustained support throughout the years from NASA for the ECCO project is gratefully acknowledged.

AUTHORS

An T. Nguyen (atnguyen@ices.utexas.edu) is Senior Research Scientist, Victor Ocaña is Research Associate, and Vikram Garg is Postdoctoral Researcher, all at the Institute of Computational Engineering and Sciences, The University of Texas at Austin, Austin, TX, USA. Patrick Heimbach is Fellow, W.A. “Tex” Moncrief Jr. Endowed Chair III in Simulation-Based Engineering Sciences, Institute for Computational Engineering and Sciences; Research Professor, Institute for Geophysics; and Associate Professor, Jackson School of Geosciences, The University of Texas at Austin, Austin, TX, USA. John M. Toole is Senior Scientist, and Richard A. Krishfield is Senior Research Specialist, both at Woods Hole Oceanographic Institution, Woods Hole, MA, USA. Craig M. Lee is Senior Principal Oceanographer, and Luc Rainville is Principal Oceanographer, both at the Applied Physics Laboratory, University of Washington, Seattle, WA, USA.

ARTICLE CITATION

Nguyen, A.T., V. Ocaña, V. Garg, P. Heimbach, J.M. Toole, R.A. Krishfield, C.M. Lee, and L. Rainville. 2017. On the benefit of current and future ALPS data for improving Arctic coupled ocean-sea ice state estimation. *Oceanography* 30(2):69–73, <https://doi.org/10.5670/oceanog.2017.223>.